

LA-UR -82-1055

MASTER

CONF-820429--4

Los Alamos National Laboratory is operated by the University of California for the United States Department of Energy under contract W-7405-ENG-36

LA-UR--82-1055

DE82 014045

TITLE: TWO-DIMENSIONAL SPATIAL-DISCRETIZATION METHODS ON A  $\frac{1}{2}$  LAGRANGIAN MESH

AUTHOR(S): Thomas R. Hill and Richard R. Paternoster

SUBMITTED TO: Los Alamos/CEA Applied Physics Conference,  
Paris, France, April 19-23, 1982

DISCLAIMER

This work was prepared as an account of work sponsored by the United States Government. It is not to be distributed outside the Government. The Government is authorized to reproduce and distribute reprints for government purposes, not withstanding any copyright notation that may appear hereon. The views and opinions contained herein are those of the author(s) and do not necessarily represent those of the United States Government.

DISTRIBUTION OF THIS DOCUMENT IS UNLIMITED

By acceptance of this article, the author recognizes that the U.S. Government retains a nonexclusive, royalty-free license to publish or reproduce the published form of this contribution, or to allow others to do so, for U.S. Government purposes.

The Los Alamos National Laboratory requests that the publisher identify this article as work performed under the auspices of the U.S. Department of Energy

Los Alamos Los Alamos National Laboratory  
Los Alamos, New Mexico 87545

## TWO-DIMENSIONAL SPATIAL-DISCRETIZATION METHODS ON A LAGRANGIAN MESH

Thomas R. Hill and Richard R. Paternoster  
Los Alamos National Laboratory  
Los Alamos, New Mexico, U.S.A.

Methods for efficiently solving the two-dimensional multigroup transport equation for orthogonal  $(x,y)$  or  $(r,z)$  geometries are generally well-developed. The extension to regular triangular meshes in  $(x,y)$  and  $(r,z)$  geometries has been done. However, some complex geometries cannot be accurately described with these methods. Furthermore, it is often desirable to couple neutronics with hydrodynamics calculations. It is desirable to perform the neutronics calculations directly on a distorted Lagrangian mesh, rather than mapping the material properties onto an orthogonal mesh. This paper will describe some of the Los Alamos work on solving the transport equation on an arbitrary Lagrangian mesh, with emphasis on the spatial differencing schemes used.

The angular variable is treated by the standard discrete-ordinates approximation, using the diamond-difference approximation for curved geometry. Before the calculation is begun, a large (packed) ordering array of size: (number of spatial mesh cell  $\times$  number of discrete-ordinates directions) is computed to specify the order of sweeping the mesh cells for each direction. This can be done in a very efficient fashion for near-spherical meshes.

By writing a conservation equation for each triangular or quadrilateral mesh cell, and using additional diamond-difference-like relationships, depending upon the number of sides visible, an equation for the cell-centered angular flux can be derived. This scheme suffers from the same difficulties as the standard diamond difference in orthogonal geometries, in addition to other deficiencies unique to Lagrangian meshes. Schemes for fix-ups of negative fluxes and boomerangs will be described. Two temporary triangular subzoning schemes will be outlined.

## TWO-DIMENSIONAL SPATIAL DISCRETIZATION METHODS ON A LAGRANGIAN MESH

### INTRODUCTION

Because of the ability to model complex geometries and the occasional interest in coupling neutronics to hydrodynamics calculations, such as in reactor safety problems, the solution of the neutron transport equation on an arbitrary Lagrangian mesh is sometimes desired.

In the past, this was most often done by mapping the material properties onto an orthogonal mesh and performing the neutronics calculation with those well-developed methods.<sup>1,2</sup> Because of the expense of this mapping and a corresponding reduction in accuracy, an effort was undertaken at Los Alamos for a direct solution of the discrete-ordinates transport equation on Lagrangian meshes. Preceding and paralleling this effort was the work at Lemaitre by Mordant.<sup>3,4</sup> In describing the Los Alamos work in this paper, emphasis will be placed on the differences between the two approaches, primarily in the spatial differencing scheme.

The Los Alamos method is based upon the constraints:

1. The method must be able to solve large meshes (> 10 000 mesh cells), so that a scheme efficient in core storage is required, and
2. The method must be able to do time dependent problems, so that a computationally-efficient and fast scheme is required.

These two restrictions resulted in a method somewhat simpler, and certainly far less elegant, than that of Mordant.

### TRANSPORT EQUATION

The angle and energy variables of the two-dimensional transport equation in (x,y) or (r,z) geometry are treated by the standard discrete ordinates and multigroup approximation,<sup>2</sup> including the truncated expansion of the scattering function in spherical harmonics.

Using the standard nomenclature of TWOTRAN,<sup>2</sup> the conservation equation for the single Lagrangian mesh cell shown in Fig. 1, for discrete-ordinates direction  $\Omega_m = (\mu_m, \eta_m)$ , can be written

$$f_1 \psi_1 + f_2 \psi_2 + f_3 \psi_3 + f_4 \psi_4 + \frac{A}{w_m} (\alpha_{m+\frac{1}{2}} \psi_{m+\frac{1}{2}} - \alpha_{m-\frac{1}{2}} \psi_{m-\frac{1}{2}}) + \sigma V \psi = SV \quad (1)$$

where

$$f_i = \begin{cases} \mu \Delta y - \eta \Delta x & (x, y) \\ \bar{r}(\mu \Delta z - \eta \Delta r) & (r, z) \end{cases} =$$

flow area on i'th face of mesh cell, with

$$f_i = \begin{cases} > 0 & \text{for outflow} \\ < 0 & \text{for inflow} \end{cases} ,$$

$$V = \text{mesh cell volume} = \begin{cases} \iint dx dy & \text{in } (x, y) \\ \iint r dr dz & \text{in } (r, z) \end{cases} ,$$

$A = \text{mesh cell area} = \iint dr dz \text{ in } (r, z)$  , and

$S = \text{mesh cell source, including scattering and fission.}$

Equation (1) may easily be applied to triangles by setting the appropriate  $f_i = 0$ .

The curvature coefficients,  $\alpha_{m \pm \frac{1}{2}}$ , satisfy the standard recursion relation<sup>2</sup> in  $(r, z)$  geometry, and are zero for  $(x, y)$  geometry, with the notation  $\alpha_m = \alpha_{m+\frac{1}{2}} + \alpha_{m-\frac{1}{2}}$ . The step approximation in angle<sup>2</sup> is used in  $(r, z)$  geometry for the first angle on each  $\eta$  level.

The diamond-difference approximation in angle is used

$$\psi_{m+\frac{1}{2}} = 2 \psi - \psi_{m-\frac{1}{2}} ,$$

so that Eq. (1) can be written

$$\psi = \frac{SV + \text{Inflows} + \frac{A}{w_m} (\alpha_{m+\frac{1}{2}} - \alpha_{m-\frac{1}{2}}) \psi_{m-\frac{1}{2}}}{\sigma V + \text{Outflows} + 2 \frac{A}{v_m} \alpha_{m+\frac{1}{2}}} \quad (2a)$$

or for the first angle on an  $\eta$ -level

$$\psi = \frac{SV + \text{Inflows}}{\sigma V + \text{Outflows} + \frac{\alpha_{m+\frac{1}{2}}}{w_m} A} \quad (2b)$$

## SPATIAL DIFFERENCING

The conservation equation scheme of Eq. (2) is based on mesh-cell edge fluxes (as opposed to a corner flux scheme). The diamond difference scheme, used so successfully in orthogonal geometries, can easily be generalized to these nonorthogonal Lagrangian meshes.

The number of known and unknown angular fluxes in Eq. (1) depends upon the orientation of the mesh cell with respect to the discrete ordinate direction. For a quadrilateral cell with  $N$  sides visible ( $N = 1, 2$ , or  $3$ ), there are  $5-N$  unknown fluxes so that  $5-N-1$  auxiliary diamond-difference like equations must be assumed to supplement the conservation Eq. (1). These supplemental equations and the resultant cell-center flux equation for the five possible cases are shown in Fig. 2.

Because of the sign on the flow areas ( $-$  for inflow,  $+$  for outflow), the equations for the cell-center fluxes in Fig. 2 are seen to be positive, provided the sources are positive. These diamond-difference like equations suffer the same defects of those in orthogonal geometries; namely, that the diamond difference extrapolations can (and do) yield negative fluxes. The appropriate equations for a set-to-zero flux fixup<sup>2</sup> are detailed in Fig. 3.

Other defects exist for this diamond-difference scheme. As one side of a quadrilateral is squeezed down to zero, the difference equation does not go over to the equation for the corresponding triangle.

Moreover, as the orientation of a mesh cell is changed from one side visible to two sides visible to three sides visible, the difference equations are not continuous from one orientation to the other. Although this is primarily an aesthetic objection, it may only mean that quantities do not converge monotonically with increasing  $S_N$  order. In time-dependent problem, this may introduce nonphysical jumps in the temporal behavior of the flux in a cell.

Although neither of these two defects exist for the step scheme, efforts to correct them for the diamond-difference scheme have not been successful.

For problems that are picked up from Lagrangian hydrodynamics, the meshes occasionally contain boomerangs and bowties. Since boomerangs are mesh cells with reentrant boundaries, a rigorous solution must reflect the solution in the adjacent cells, destroying the explicitness of the scheme. Several ad hoc fixups are shown in Fig. 4. Generally, the number of boomerangs in a mesh are few, so that a crude treatment of these cells has little effect on the overall solution. No satisfactory treatment for bowties has been devised yet.

## ALTERNATIVE DIFFERENCE SCHEMES

The step approximation in the lateral direction for one-side visible quadrilaterals (see Fig. 2) is obviously a crude approximation. In order to get the proper slope to the cell flux distribution in this lateral direction, a scheme for this one-side visible case, based on Carlson's method of characteristics<sup>5</sup>, was examined. The lateral cell edge fluxes are distributed based on the

distance of the cell edge midpoints from a plane perpendicular to the beam through the center of the cell, as diagrammed in Fig. 5. However, because of its complicated nature and the limited improvements in accuracy it offered, this scheme was abandoned.

After taking statistics on a number of spherical-like meshes, it was noted that the vast majority of the cell solutions were for the two-side visible case, ranging from 95% for exactly spherical meshes to a low of 85% for one highly-distorted mesh. The remaining cells solutions were roughly evenly distributed between the other four cases (one side and three side visible quadrilaterals, and one and two side visible triangles). Thus, improvements in these four latter schemes will probably only produce marginal improvements in overall results.

Two more accurate diamond difference-like have been examined. One is a temporary triangular zoning scheme in which the quadrilateral is arbitrarily divided into two triangles, as outlined in Fig. 6 for a two-side visible case. The other was a temporary triangular fine zoning scheme in which the quadrilateral is divided into four triangles, as outlined in Fig. 7.

Although both of these schemes yielded some improvements in accuracy, it was felt the improvement did not justify the additional compute costs. The only quantity saved between iterations was the cell-centered flux, so that the new scattering and fission sources are only the cell-averaged values. Thus, these crudely-approximated sources degrade the improved accuracy resulting from a more accurate difference scheme.

#### THE LAMEDOC CODE

The LAMEDOC (Lagrangian Mesh Discrete Ordinates Transport Code) has been developed at Los Alamos to solve the discrete-ordinates transport equation on an arbitrary Lagrangian mesh. Much of the structure is the same as in the TWOTRAN code.<sup>2</sup> LAMEDOC is only a methods testing code, with much un-optimized coding, and not a usable production code in any sense.

In addition to the spatial differencing scheme, the second major problem not found in orthogonal-mesh codes is how to sweep the Lagrangian mesh. For a given discrete-ordinate direction, the order of solving the mesh cells is not, a priori, known. A number of iterative schemes for sweeping the mesh were examined. Though highly optimized, they were found to be not competitive (except for pure absorbing systems) with an explicit scheme of sweeping the mesh.

Although being computationally efficient, an explicit sweeping scheme requires a considerable core storage overhead, namely, an ordering array of the size of one angular flux array. This ordering array specifies the order in which the spatial mesh is to be swept for each discrete ordinate direction. It is computed at the start of the problem by testing the sign of the flows between each mesh cell until a (non-unique) ordering is obtained. By assuming a banded structure, as shown in Fig. 8, this ordering array can be computed quite efficiently. For time-independent problems, the overhead for computing this ordering array is negligible. For time-dependent problems, this overhead

becomes significant. However, the ordering array from the previous time-step can be used to compute the ordering array for the present time step fairly efficiently.

LAMEDOC uses the traditional three level of iterations: inner iterations on the within-group scatter source, outer iterations on the fission source for eigenvalue  $\lambda$ , and alpha iterations for the time-absorption eigenvalue  $\alpha$ . Both the inner and outer iterations are accelerated by a material mesh variant of the standard coarse-mesh rebalance.<sup>2</sup>

The  $\alpha$  iterations are also accelerated with a group-collapsed material mesh rebalance.<sup>6</sup> The  $\alpha$  iterations on the multigroup transport equation can be written as

$$L\psi^\ell + (\Sigma + V^{-1} \alpha^{\ell-1}) \psi^\ell = S\psi^\ell + \frac{1}{\lambda^\ell} F\psi^\ell, \quad (3)$$

where  $L$  is the leakage operator,  $\Sigma$  a diagonal matrix of macroscopic total cross sections,  $V^{-1}$  is a diagonal matrix of inverse group speeds,  $S$  and  $F$  are the scattering and fission operators, and  $\lambda$  the intermediate eigenvalue. The solution of Eq. (3) for the eigenvalue  $\alpha$ , with  $\lambda = 1$ , is sought. Multiplying the fluxes  $\psi$  in Eq. (3) by material-mesh dependent rebalance factors,  $f_k$ , and integrating over all angles and energy groups and mesh cells in material-mesh zone  $k$  yields a matrix equation for the eigenvalue  $\alpha$  and eigenvector of rebalance factors.

$$[FL + AB - FS] f = -\alpha FV f, \quad (4)$$

where  $AB$ ,  $FS$ , and  $FV$  are diagonal matrices

$$AB_k = \int_k dV \int dE \Sigma_a \phi, \quad$$

$$FS_k = \int_k dV \int dE v \Sigma_f \phi, \quad$$

$$FV_k = \int_k dV \int dE \frac{1}{v} \phi, \quad$$

and  $FL$  is a full material-mesh flow matrix.

The eigenvalue spectrum of Eq. (4) ranges from the desired largest, positive eigenvalue to negative infinity. Thus, the simple power iteration used for the outer material-mesh rebalance will not produce the desired eigenvalue. The inverse power iteration scheme has been found to be effective in solving Eq. (4).

Various convergence tests are used on the different levels of iterations in LaMEDOC. During the early iterations when  $\alpha$  is not accurately known, it makes little sense to converge the iterations very tightly. Consequently, LaMEDOC uses a variable convergence precision scheme in which the various levels of iteration are converged to a precision given by the ad hoc recipe:

$$\varepsilon = 10^{-2} (1 - \lambda) + \lambda \varepsilon_{\text{final}} ,$$

where  $\varepsilon_{\text{final}}$  is the desired, final convergence precision, a user-specified parameter. For some problems with much scattering, this scheme can cause the  $\alpha$  eigenvalue iterations to diverge, but works well for highly-absorbing systems.

Occasionally, it is desired to compute  $\alpha$  eigenvalues for subcritical systems. LaMEDOC contains an algorithm<sup>7</sup> to obtain these very difficult eigenvalues that succeeds when other transport codes fail.

#### NUMERICAL RESULTS

LaMEDOC has been used successfully on a variety of problems. Good agreement has been obtained with results from the ONETRAN<sup>8</sup> and TWOTRAN codes for problems that can be modeled exactly on those codes. The defects described above in the spatial differencing have not appeared to be a serious difficulty in any problem yet computed. Many problems make frequent use of the negative-flux fixup scheme. If the cell-centered fluxes are the only quantity examined, the negative fluxes and the spatial oscillations of the cell-edge fluxes are not evident.

For steady-state problems when integral quantities are desired, such as eigenvalues, absorption rates, and leakages, the crudeness of the diamond-difference scheme appears to be no impediment to its use. In time dependent problems when localized sources may be present and large spatial flux gradients may exist, the diamond-difference scheme may prove to be inadequate.

Figure 9 shows a spherical problem consisting of a pure <sup>235</sup>U sphere, surrounded by a beryllium reflector. The results from LaMEDOC for this problem are shown in Table 1 for a series of spatial meshes. Even for the coarse spatial mesh b, the eigenvalue  $\alpha$  is in error by less than 1%.

The important parameter in comparing the computing efficiency of various spatial differencing schemes is

$$T = \frac{\text{Total CPU time}}{(\# \text{ of groups}) (\# \text{ of mesh cells}) (\# \text{ of directions}) (\# \text{ of inners})} .$$

For this problem, LaMEDOC appears to have a T of about 15  $\mu$ s. This quantity is, of course, a strong function of coding efficiency, compiler optimization, and the computing facilities software.



#### REFERENCES

1. B. G. Carlson and K. D. Lathrop, "Transport Theory-The Method of Discrete Ordinates," Computing Methods in Reactor Physics, H. Greenspan, C. N. Kelber, and D. Okrent, Eds. (Gordon and Breach, New York, 1968).
2. K. D. Lathrop and F. W. Brinkley, "TWOTRAN-II: An Interfaced, Exportable Version of the TWOTRAN Code for Two-Dimensional Transport," LA-4348-MS (July 1973).
3. M. Mordant, "ZEPHYR: A Code for Solving Neutron Transport Problems on Irregular Meshes in Two-Dimensional Geometries," IAEA meeting Bologna, Italy, November 3-5, 1975.
4. M. Mordant, "Some Efficient Lagrangian Mesh Finite Elements Encoded in ZEPHYR for Two-Dimensional Calculations," Annals of Nucl. Eng., 8 (1981), p. 657-675.
5. B. Carlson, "A Method of Characteristics and Other Improvements in Solution Methods for the Transport Equation," Nucl. Sci. & Eng., 61 (1976), p. 416.
6. T. R. Hill and W. F. Miller, Jr., "Rebalance Acceleration of Time Absorption Eigenvalue Searches," accepted for publication in Trans. Am. Nucl. Soc., 40 (June 1982).
7. T. R. Hill, "Time Absorption Eigenvalue Searches for Subcritical Systems," Trans. Am. Nucl. Soc., 39 (December 1981).
8. T. R. Hill, "ONETRAN: A Discrete Ordinates Finite Element Code for the Solution of the One-Dimensional Multigroup Transport Equation," Los Alamos Scientific Laboratory report LA-5990-MS (June 1973).

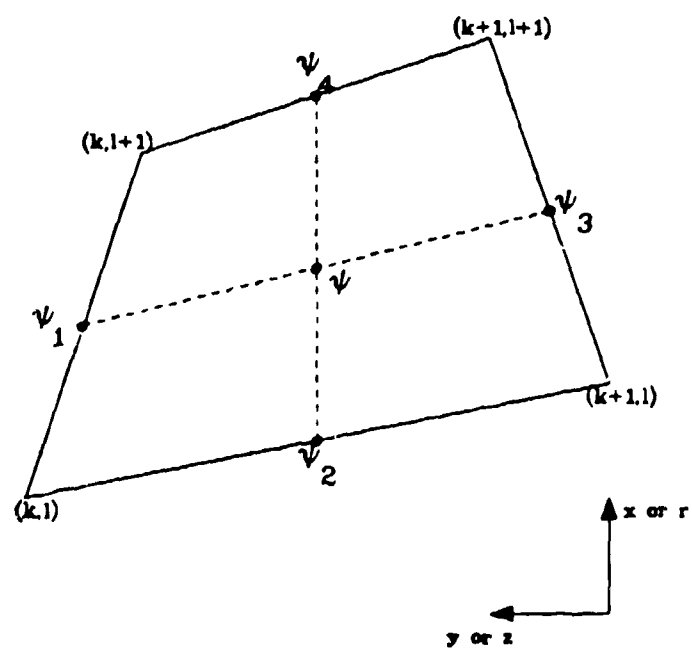


FIGURE 1. Lagrangian Mesh Cell

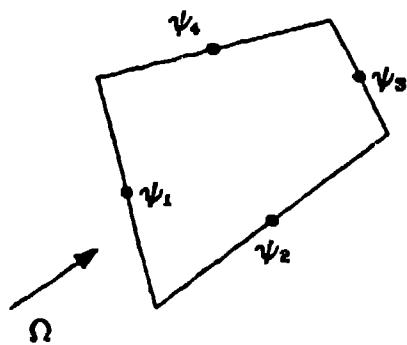
Table 1. LaMEDOC Problem A Results

6 Groups,  $S_6$  Quadrature,  $\varepsilon = 10^{-4}$

	Mesh	Total	CDC 7600		
	Cells	Inners	CPU Time	$T^b$	$\alpha^a$
Mesh			s	$\mu s$	gen/sh
a	16	465	16.26	15.1	2.1123
b	64	497	67.64	14.8	0.8461
c	256	537	302.19	15.3	0.8544
d	1024	545	1569.86	19.5	0.8562

a ONETRAN  $\alpha$  ( $S_{16}$ , 200 mesh cells) = 0.8565

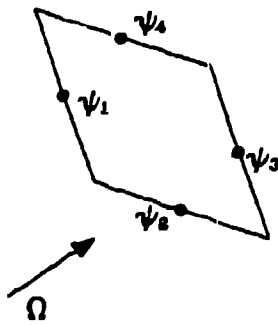
b  $T$  = CDC 7600 CPU Time per group per mesh cell  
per direction per inner iteration



One Side Visible :  $\psi_1$  known

$$\psi_2 = \psi_4 = \psi \quad \psi_3 = 2\psi - \psi_1$$

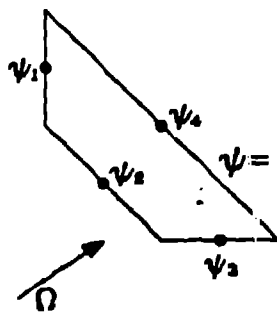
$$\psi = \frac{SV - (f_1 - f_3)\psi_1 + A\alpha_m \psi_{m-1/2}/w_m}{2f_3 + f_2 + f_4 + \sigma V + 2A\alpha_{m+1/2}/w_m}$$



Two Sides Visible :  $\psi_1, \psi_2$  known

$$\psi_3 = 2\psi - \psi_1 \quad \psi_4 = 2\psi - \psi_2$$

$$\psi = \frac{SV - (f_1 - f_3)\psi_1 - (f_2 - f_4)\psi_2 + A\alpha_m \psi_{m-1/2}/w_m}{2f_3 + 2f_4 + \sigma V + 2A\alpha_{m+1/2}/w_m}$$

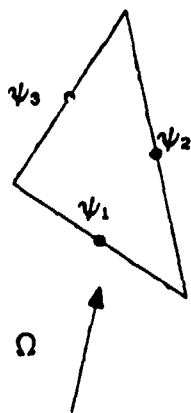


Three Sides Visible :  $\psi_1, \psi_2, \psi_3$  known

$$\psi_4 = 4\psi - \psi_1 - \psi_2 - \psi_3$$

$$\psi = \frac{SV - (f_1 - f_4)\psi_1 - (f_2 - f_4)\psi_2 - (f_3 - f_4)\psi_3 + A\alpha_m \psi_{m-1/2}/w_m}{4f_4 + \sigma V + 2A\alpha_{m+1/2}/w_m}$$

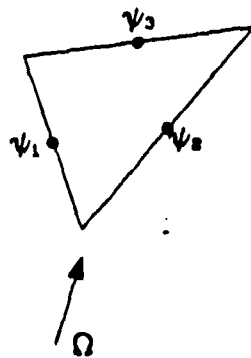
FIGURE 2a. Quadrilateral Diamond Difference



One Side Visible :  $\psi_1$  known

$$\psi_2 = \psi_3 = (3\psi - \psi_1)/2$$

$$\psi = \frac{SV - (f_1 - f_3/2 - f_2/2)\psi_1 + A\alpha_m\psi_{m-1/2}/w_m}{3f_2/2 + 3f_3/2 + \sigma V + 2A\alpha_{m+1/2}/w_m}$$

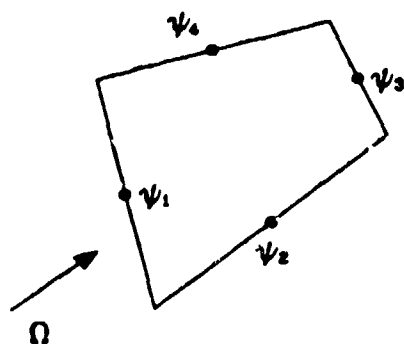


Two Sides Visible :  $\psi_1$  ,  $\psi_2$  known

$$\psi_3 = 3\psi - \psi_1 - \psi_2$$

$$\psi = \frac{SV - (f_1 - f_3)\psi_1 - (f_2 - f_3)\psi_2 + A\alpha_m\psi_{m-1/2}/w_m}{3f_3 + \sigma V + 2A\alpha_{m+1/2}/w_m}$$

FIGURE 2b. Triangle Diamond Difference

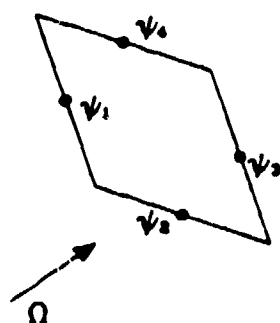


One Side Visible :  $\psi_1$  known

Suppose  $\psi_3 < 0$

Set  $\psi_2 = \psi_4 = \psi$  and  $\psi_3 = 0$

$$\psi = \frac{SV - f_1\psi_1 + A\alpha_m\psi_{m-1/2}/w_m}{f_2+f_4 + \sigma V + 2A\alpha_{m+1/2}/w_m}$$

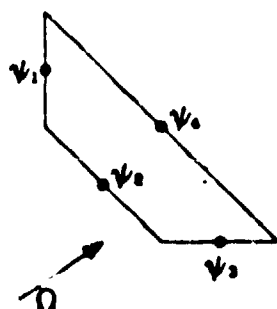


Two Sides Visible :  $\psi_1, \psi_2$  known

Suppose  $\psi_4 < \psi_3 < 0$

Set  $\psi_4 = 0$  and  $\psi_3 = 2\psi - \psi_1$

$$\psi = \frac{SV - f_2\psi_2 - (f_1 - f_3)\psi_1 + A\alpha_m\psi_{m-1/2}/w_m}{2f_3 + \sigma V + 2A\alpha_{m+1/2}/w_m}$$



Three Sides Visible :  $\psi_1, \psi_2, \psi_3$  known

Suppose  $\psi_4 < 0$

Set  $\psi_4 = 0$

$$\psi = \frac{SV - f_1\psi_1 - f_2\psi_2 - f_3\psi_3 + A\alpha_m\psi_{m-1/2}/w_m}{\sigma V + 2A\alpha_{m+1/2}/w_m}$$

FIGURE 3a. Quadrilateral Flux Fixup

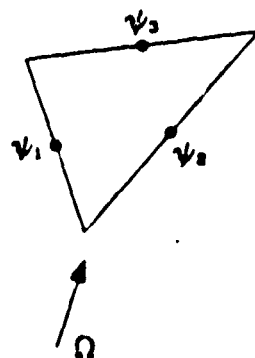


One Side Visible :  $\psi_1$  known

Suppose  $\psi_2 = \psi_3 < 0$

Set  $\psi_2 = \psi_3 = 0$

$$\psi = \frac{SV - f_1\psi_1 + A\alpha_m\psi_{m-1/2}/w_m}{\sigma V + 2A\alpha_{m+1/2}/w_m}$$



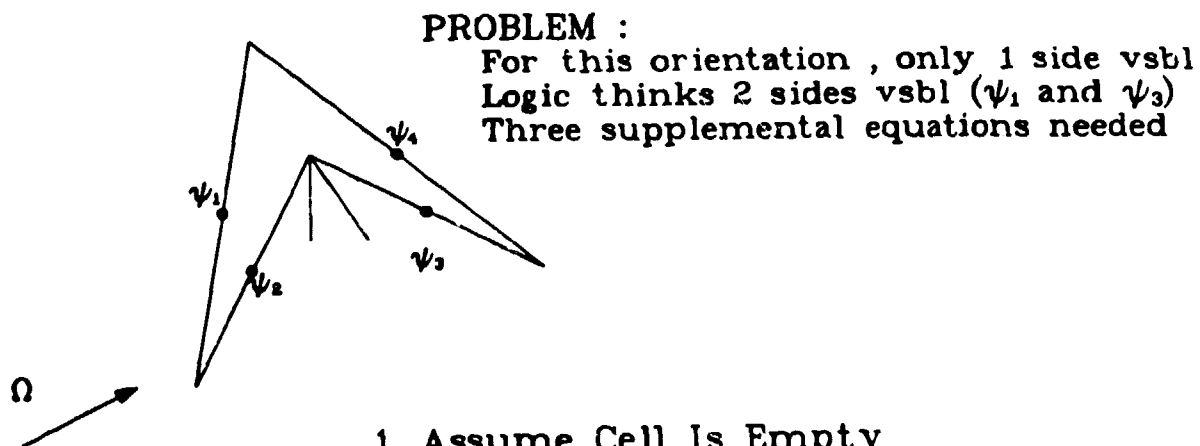
Two Sides Visible :  $\psi_1, \psi_2$  known

Suppose  $\psi_3 < 0$

Set  $\psi_3 = 0$

$$\psi = \frac{SV - f_1\psi_1 - f_2\psi_2 + A\alpha_m\psi_{m-1/2}/w_m}{\sigma V + 2A\alpha_{m+1/2}/w_m}$$

FIGURE 3b. Triangle Flux Fixup



1. Assume Cell Is Empty

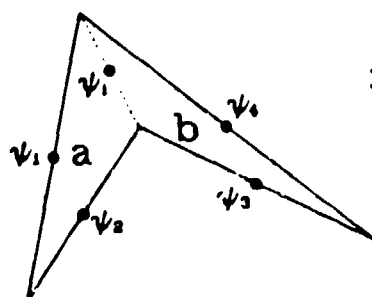
$$\psi = \psi_1 \quad \text{and} \quad \psi_2 = \psi_4 (= \psi_3) = \psi$$

2. Use Step Approximation

$$\psi_2 = \psi_3 = \psi_4 = \psi$$

$$\psi = \frac{SV - f_1\psi_1 + A\alpha_m\psi_{m-1/2}/w_m}{f_2+f_3+f_4 + \sigma V + 2A\alpha_{m+1/2}/v_{in}}$$

$f_2f_4 > 0, f_3 < 0$  Denominator can vanish



3. Temporary Triangulation

Solve  $\Delta a$  (1 side vsbl) for  $\psi_a, \psi_2, \psi_1$

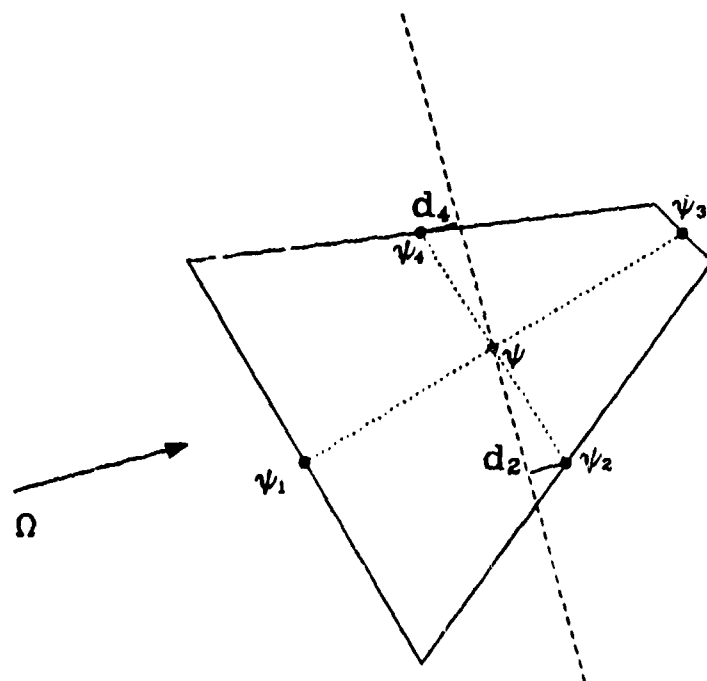
Solve  $\Delta b$  (2 sides vsbl) for  $\psi_b, \psi_4$

by assuming  $\psi_3 = \psi_2$

$$\text{Set } \psi = (\psi_a V_a + \psi_b V_b) / V$$

FIGURE 4. BOOMERANG CELL FIXUPS



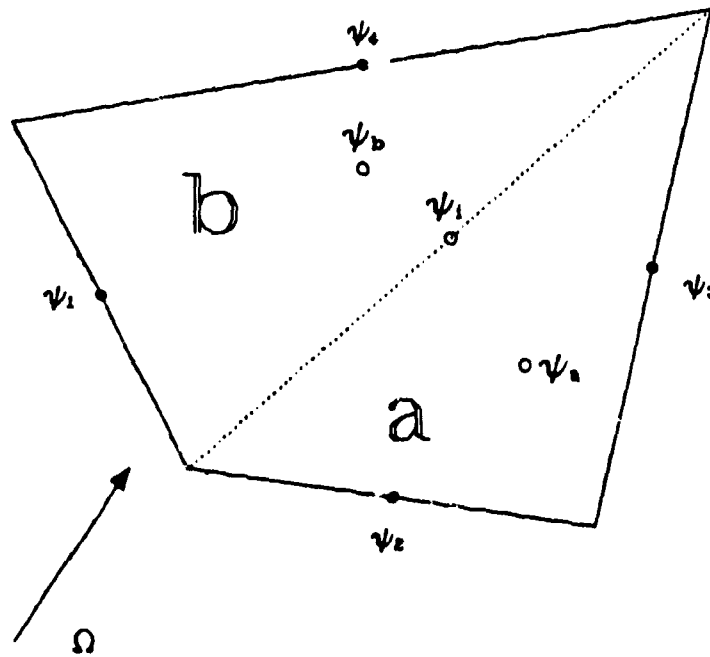


Instead of step scheme in lateral direction

$$\psi_4 = \psi_2 = \psi$$

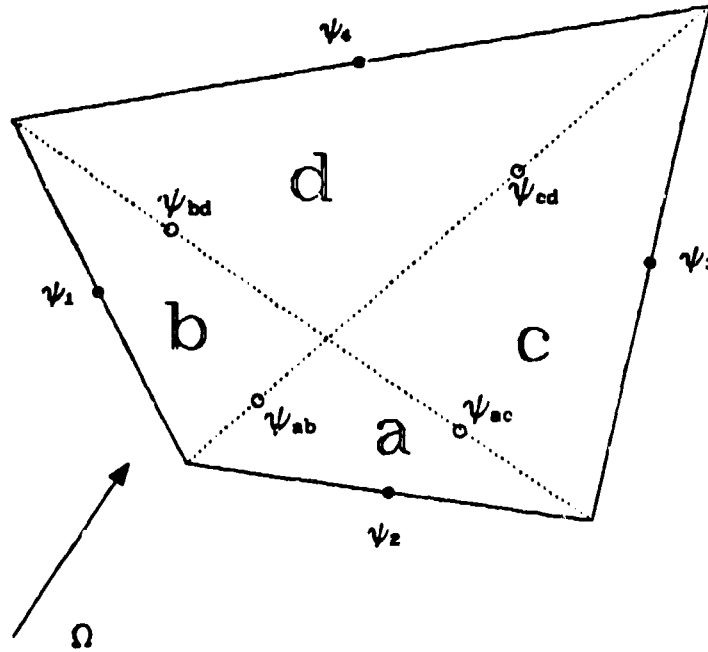
Relate  $\psi_2$ ,  $\psi_4$  to  $\psi$  based  
on  $d_2$  and  $d_4$

FIGURE 5. ONE SIDE VISIBLE ALTERNATIVE



Split quadrilateral into  $\Delta a$  and  $\Delta b$   
 Solve  $\Delta a$  (1 side vsbl) for  $\psi_a$ ,  $\psi_3$ ,  $\psi_1$   
 Solve  $\Delta b$  (2 sides vsbl) for  $\psi_b$ ,  $\psi_4$   
 Set  $\psi = (V_a\psi_a + V_b\psi_b)/V$

FIGURE 6. Temporary Triangular Zoning



Split quadrilateral into  $\Delta a$  ,  $\Delta b$  ,  $\Delta c$  ,  $\Delta d$   
 Solve  $\Delta a$  (1 side vsbl) for  $\psi_a$  ,  $\psi_{ab}$  ,  $\psi_{ac}$   
 Solve  $\Delta b$  (2 sides vsbl) for  $\psi_b$  ,  $\psi_{bd}$   
 Solve  $\Delta c$  (1 side vsbl) for  $\psi_c$  ,  $\psi_3$  ,  $\psi_{cd}$   
 Solve  $\Delta d$  (2 sides vsbl) for  $\psi_d$  ,  $\psi_4$   
 Set  $\psi = (V_a\psi_a+V_b\psi_b+V_c\psi_c+V_d\psi_d)/V$

FIGURE 7. Temporary Fine Triangular Zoning

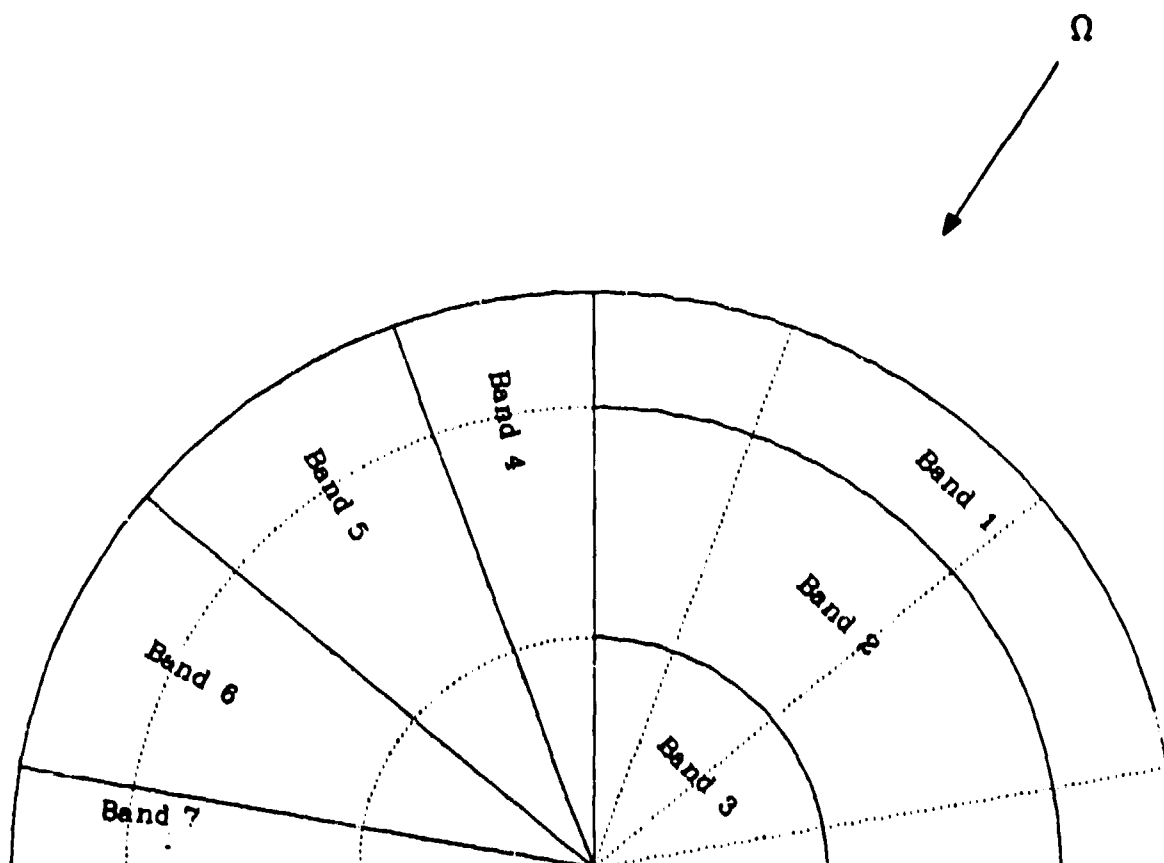
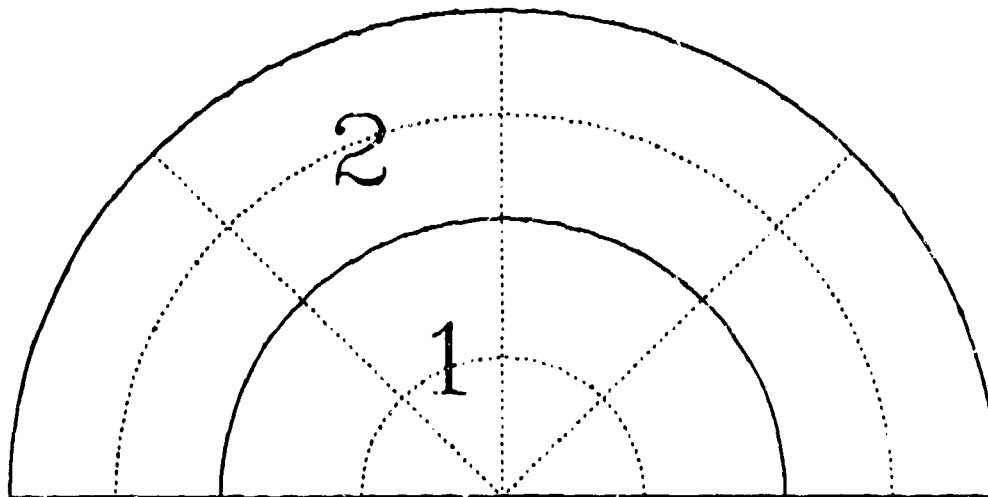


FIGURE 8. BAND STRUCTURE FOR ORDERING ARRAY



Zone 1 :                      Core  
                                  17.46 cm. radius  
                                  Pure  $^{235}\text{U}$   
                                   $\rho = 18.74 \text{ gm/cm}^3$

Zone 2 :                      Reflector  
                                  6.00 cm. thick  
                                  Pure Be  
                                   $\rho = 1.85 \text{ gm/cm}^3$

6 group Hansen-Roach Cross Sections

$S_8$  Quadrature ,  $P_0$  Scatter

Mesh :                      a. (4 angular intervals, 2 + 2 radial intervals)  
                                  b. (8 , 4+4 )  
                                  c. (16 , 8+8 )  
                                  d. (32 , 16+16 )  
                                  e. (64 , 32+32 )

FIGURE 9. LaMEDOC TEST PROBLEM A